

# We are IntechOpen, the world's leading publisher of Open Access books Built by scientists, for scientists

6,900

Open access books available

185,000

International authors and editors

200M

Downloads

Our authors are among the

154

Countries delivered to

TOP 1%

most cited scientists

12.2%

Contributors from top 500 universities



WEB OF SCIENCE™

Selection of our books indexed in the Book Citation Index  
in Web of Science™ Core Collection (BKCI)

Interested in publishing with us?  
Contact [book.department@intechopen.com](mailto:book.department@intechopen.com)

Numbers displayed above are based on latest data collected.  
For more information visit [www.intechopen.com](http://www.intechopen.com)



# New Analytical Model for Swellable Materials

*Sayyad Zahid Qamar, Maaz Akhtar and Tasneem Pervez*

*The history of science shows that theories are perishable. With every new truth that is revealed we get a better understanding of Nature, and our conceptions and views are modified.*

*Nikola Tesla*

## Abstract

As discussed in Chapter 6, numerical prediction of swelling can be attempted using existing hyperelastic material models available in commercial finite element (FE) packages. However, none of these models can accurately represent the behavior of swelling elastomers. The major shortcoming of currently available swelling models is that they consider Gaussian statistics for mechanical contribution of configuration entropy, which is based on chains having limited extensibility. Some later models (not yet incorporated into commercial FE packages) can give a reasonable account of certain behavior patterns in swelling elastomers, but do not explain other aspects well. One of the new approaches is to treat swelling elastomers as gels. As described earlier, gels are mostly liquid, yet they behave like solids due to a three-dimensional cross-linked network within the liquid. Many authors consider gel as poro-elastic or porous and use Darcy's law to model the amount of fluid influx. However, a swollen elastomer mostly consists of the solvent. When an external load is applied, maximum resistance comes from the solvent molecules as in diffusion. Also, most of the new models are quite complex in concept and formulation, and there is a serious need for a scientifically simpler model.

**Keywords:** swelling elastomer, new material model, continuum mechanics, non-Gaussian statistics

## 1. Introduction

As discussed in Chapter 6, numerical prediction of swelling can be attempted using existing hyperelastic material models available in commercial finite element (FE) packages. However, none of these models can accurately represent the behavior of swelling elastomers [1]. The major shortcoming of currently available swelling models is that they consider Gaussian statistics for mechanical contribution of configuration entropy, which is based on chains having limited extensibility [2]. These models assume small stretch of elastomer chains, while swelling elastomers experience much larger stretches. That is why they show only modest agreement with experimental data.

Some later models (not yet incorporated into commercial FE packages) can give a reasonable account of certain behavior patterns in swelling elastomers, but do not

explain other aspects well [3]. One of the new approaches is to treat swelling elastomers as gels. As described earlier, gels are mostly liquid, yet they behave like solids due to a three-dimensional cross-linked network within the liquid. Many authors consider gel as poro-elastic or porous and use Darcy's law to model the amount of fluid influx. However, a swollen elastomer mostly consists of the solvent. When an external load is applied, maximum resistance comes from the solvent molecules as in diffusion. Also, most of the new models are quite complex in concept and formulation, and there is a serious need for a scientifically simpler model.

## 2. Proposed model: salient features

Presented below is the development of a new material model for the prediction of swelling in elastomeric materials, using a continuum mechanics approach. To account for the changes in configuration entropy of the elastomer chains due to swelling, almost all available models [4–7] use classical Gaussian-statistics in which chains are considered to have limited extensibility [8]. Swelling elastomers undergo large deformations as the chain network stretches more. More realistic non-Gaussian statistics is therefore used for model development here, to account for large mechanical stretches, in terms of mechanical contribution of configuration entropy.

It was concluded in Chapter 6 that Ogden model gives the closest predictions for swelling elastomers [1]. The hyperelastic portion of the new model is therefore based on the phenomenological stretch-based Ogden model. This second-order non-Gaussian strain energy function is used to define changes due to configuration entropy [9]. Rather than treating swelling as an osmosis problem, diffusion is considered to be the mechanism responsible for fluid influx. Flory-Huggins theory is used for incorporating the thermodynamics of mixing of polymer and solvent (absorption of fluid into the elastomer). Unlike other models, which consider only some of the pertinent parameters, proposed model includes most of the relevant material and structural properties of the elastomer, and environmental conditions (temperature, water salinity, coefficient of diffusion, polymer-solvent interaction parameter, etc).

The formulation is based on thermodynamically consistent diffusion-deformation theory for elastomer gels considering the interaction and mixing of polymer and solvent. Solid and liquid like chemical species are considered as a single homogenized continuum [7, 10]. It is assumed that Helmholtz free energy can be divided into network stretching and Fluid-polymer mixing [11]. Flory-Huggins theory is used to describe the changes in entropy due to solid–fluid mixing.

Fluid imbibition in swelling elastomers follows the mechanism of diffusion [4, 12]. Diffusion equations are formulated through suitable balance laws for fluid content. Coefficient of diffusion ( $D$ ) for fluid molecules is assumed to be isotropic and independent of deformation gradient. As fluid molecules form a majority portion of the swollen elastomer, this simplification seems quite realistic. Deformation due to swelling may occur in two ways, short range or long range, as shown in **Figure 1**. Initially, the solvent molecules diffuse and re-arrange so that shape changes but volume remains constant. In long-range motion, gel changes shape as well as volume. It is assumed in developing the model that amount of solvent only transports when change of volume occurs, and it remains constant when elastomer undergoes only change of shape.

Swelling elastomers are assumed to be incompressible because they possess high bulk modulus and low shear modulus [13]. Change in volume is negligible as

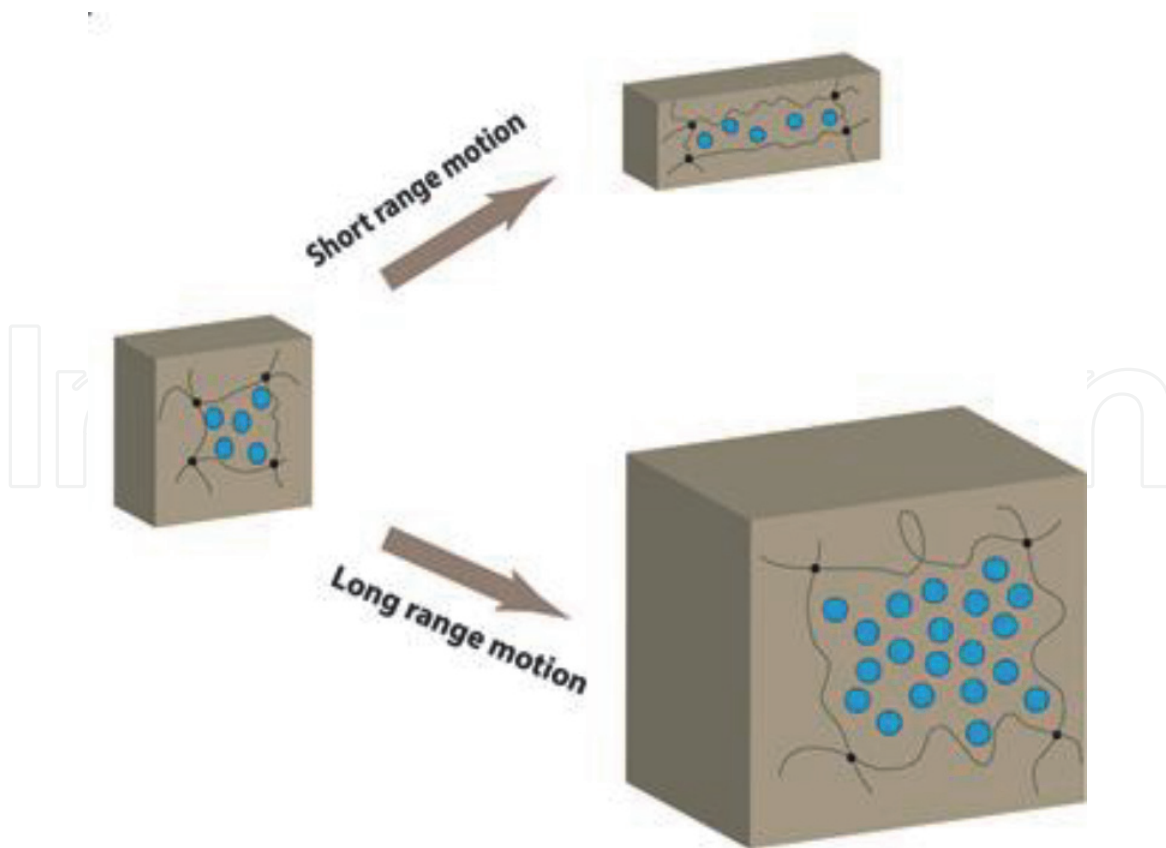


**Figure 1.**  
 Deformation under long and short range motion of gel.

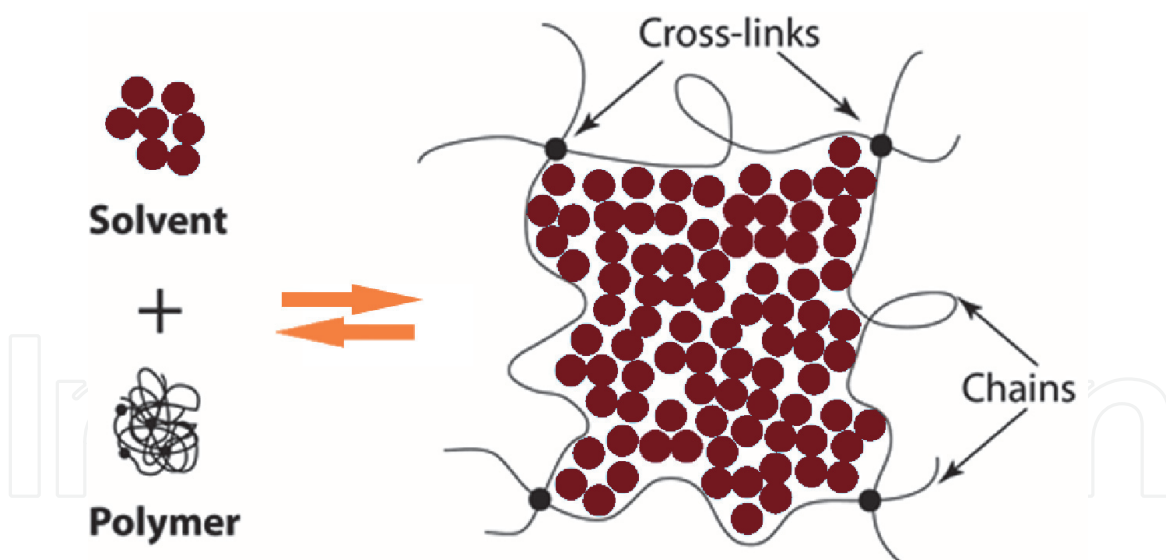


**Figure 2.**  
 Imbibition of solvent and stretching of chain.

compared to shape change. Gels are soft materials that can deform easily and can undergo volume changes equal to several times its initial volume. This change in volume occurs only as a result of imbibition of solvent molecules. It should be noted that volume of swollen elastomer is the state bounded by material points that deform with the elastomer chains. Swelling of gel actually means deformation of the elastomer network. When a swellable elastomer is placed in a solvent, it absorbs it, resulting in stretching of chains with increase in volume; **Figure 2**. This unique feature necessitates the consideration of large deformation and helps in developing the mathematical basis for mechanics of swelling. Mathematical structure used to

derive deformation of elastomer network due to swelling is similar to the approach used in rubber elasticity. Rubber can be treated as a special case of swelling elastomer with no fluid. Succeeding sections describe the continuum mechanics theory for swelling elastomers.

### 3. Proposed model: mathematical formulation

The new model for swelling in elastomers is developed in this section, describing the relevant contributions of kinematics, force equilibrium, solvent equilibrium, system free energy, kinematic constraint for network incompressibility, kinetics, and thermodynamics of mixing.

#### 3.1 Kinematics

Polymer-fluid mixture is considered to be a single homogenized continuum body permitting diffusion of solvent. Reference configuration is a three dimensional dry state of elastomer represented by  $\Omega_0$  contained within a surface denoted by  $S_0$ . Current configuration represents the deformed swollen state of elastomer network. Intermediate or auxiliary state is the local distortion of elastomer because of volume increase only. Later rotation and stretching of swollen elastomer gives the mechanical elastic deformation in final configuration.

Consider a particle  $A$  labeled by its position  $\mathbf{X}$  in the reference state. Deformation of entire material is described by motion and solvent concentration with smooth mapping of all material particles to the final state. After deformation, particle  $A$  attains a new position  $\mathbf{x}$  in current configuration as shown in **Figure 3**. Similarly, each particle is deformed and attains a new position in the final state.

Analytical description of the deformation of a continuum can follow either *Eulerian* (spatial) or *Lagrangian* (material) descriptions. In *Eulerian* approach, deformation is referred to the current state, while in *Lagrangian* description deformation is referred to reference configuration [14]. In continuum mechanics of solid bodies, spatial description is less beneficial since current configuration is not known. Consider particles  $A$  and  $B$  in Ref. configuration represented by positions  $\mathbf{X}_A$  and  $\mathbf{X}_B$ , respectively. Elemental vector is given by

$$d\mathbf{X} = \mathbf{X}_B - \mathbf{X}_A. \quad (1)$$

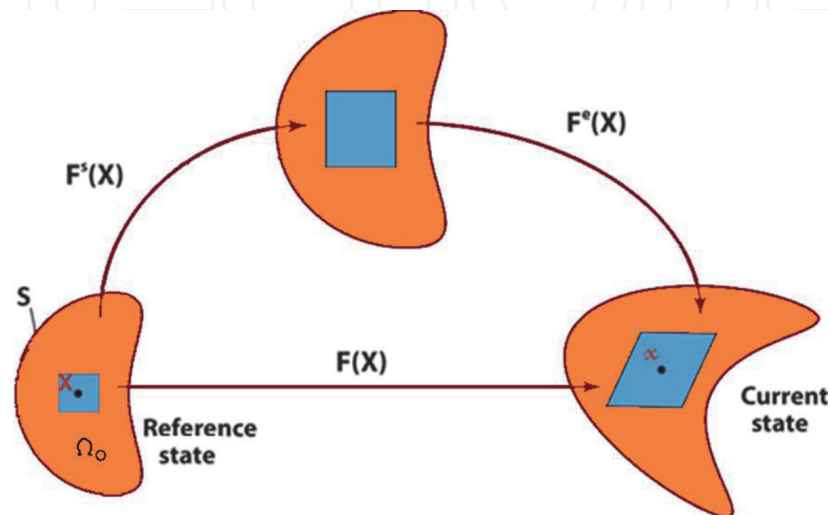


**Figure 3.** Schematic of the reference (dry), intermediate (swollen), and current (deformed) configurations.

After deformation at time ( $\mathbf{t}$ ), particles occupy spatial positions  $\mathbf{x}_A$  and  $\mathbf{x}_B$  in current configuration, having elemental vector given by

$$d\mathbf{x} = \mathbf{x}_B - \mathbf{x}_A. \quad (2)$$

Displacement of the particles  $A$  and  $B$  is given by

$$\mathbf{u}_A = \mathbf{x}_A - \mathbf{X}_A, \quad \mathbf{u}_B = \mathbf{x}_B - \mathbf{X}_B. \quad (3)$$

Displacement attained by material in the current configuration can be written as

$$\mathbf{u}(\mathbf{X}, t) = \mathbf{x} - \mathbf{X}. \quad (4)$$

Relationship between current and reference state (before and after deformation) is expressed by the *deformation gradient tensor*  $\mathbf{F}(\mathbf{X})$ , expressed as [14].

$$d\mathbf{x} = \mathbf{F} \cdot d\mathbf{X} = d\mathbf{X} \cdot \mathbf{F}^T$$

$$\mathbf{F} = \left( \frac{\partial \mathbf{x}}{\partial \mathbf{X}} \right) \text{ or } F_{ij} = \frac{\partial x_i(\mathbf{X}, t)}{\partial X_j}. \quad (5)$$

A crucial kinematic constituent of the current model is the multiplicative decomposition of the deformation gradient into swelling and mechanical elastic parts as suggested by Flory [11]. Local distortion of the material at  $\mathbf{X}$  due to swelling is given by  $\mathbf{F}^s(\mathbf{X})$ , while rotation and stretching of swollen network is specified by  $\mathbf{F}^e(\mathbf{X})$ . Hence, deformation gradient can be written as

$$\mathbf{F} = \mathbf{F}^e \mathbf{F}^s. \quad (6)$$

Jacobian  $J$  is the determinant of deformation gradient such that

$$J = \det \mathbf{F} > 0.$$

$$J^e = \det \mathbf{F}^e \quad \text{and} \quad J^s = \det \mathbf{F}^s \quad (7)$$

Using Eq. (6) and definition of Jacobin from Eq. (7), we can write

$$J = J^e J^s. \quad (8)$$

### 3.2 Force equilibrium

The principle of virtual work is considered to be a fundamental law in continuum mechanics [15]. It states that the magnitude of virtual work for the forces acting on a particle in equilibrium is zero for any arbitrary virtual motion. The balance of body forces ( $\mathbf{b}$ ) per unit volume at equilibrium in reference configuration is given by

$$\text{divs} + \mathbf{b} = 0, \quad (9)$$

where  $\mathbf{s}$  is a statically admissible stress field that holds true for any test function  $\xi$ . Multiplying Eq. (9) by this test function and integrating with respect to volume gives

$$\int_V (\text{divs} + \mathbf{b}) \xi dV = 0$$

$$\Rightarrow \int_V \xi \text{divs} dV + \int_V \mathbf{b} \xi dV = 0. \quad (10)$$

We know that

$$\operatorname{div}(\mathbf{A}\boldsymbol{\varepsilon}) = \boldsymbol{\varepsilon} \operatorname{div}\mathbf{A}^T + \operatorname{tr}(\mathbf{A} \operatorname{grad}\boldsymbol{\varepsilon}), \text{ and } \operatorname{tr}(\mathbf{A}^T\mathbf{B}) = \mathbf{A}:\mathbf{B}.$$

Eq. (10) thus becomes

$$\int_V \{ \operatorname{div}(\mathbf{s}\boldsymbol{\xi}) - \mathbf{s} : \operatorname{grad}(\boldsymbol{\xi}) + \mathbf{b} \cdot \boldsymbol{\xi} \} dV = 0. \quad (11)$$

Applying Gauss divergence theorem to first term of Eq. (11) transforms the behavior from inside the body to the vector field ( $\mathbf{n}$ ) through the surface,

$$\int_V \operatorname{div}(\mathbf{s}\boldsymbol{\xi}) dV = \int_S \mathbf{sn}\boldsymbol{\xi} dA.. \quad (12)$$

Cauchy's law states that a stress tensor exists which maps the normal to a surface into traction vector acting on the surface. When applied on Eq. (12) traction boundary loads ( $\mathbf{t}$ ) per unit area are added to the equation. Rearranging the terms gives the statement for principle of virtual work:

$$\int_V \mathbf{s}_{ij} \frac{\partial \xi_i}{\partial \mathbf{X}_j} dV = \int_V \mathbf{b}_i \xi_i dV + \int_S \mathbf{t}_i \xi_i dA = 0. \quad (13)$$

### 3.3 Solvent equilibrium

Changes in solvent concentration for any material are typically explained through diffusion across the boundary. Let  $C(\mathbf{X}, t)$  denote the concentration of solvent molecules absorbed by the polymer per unit volume of reference configuration, with the assumption that no chemical reactions occur. Solvent flux ( $\boldsymbol{\phi}$ ) per unit area represents the amount of solvent particles entering through the boundary per unit time. For all the particles, conservation of solvent molecules takes the following form [10].

$$\int_V \dot{C} dV = - \int_S \boldsymbol{\phi} \cdot \mathbf{m} dA. \quad (14)$$

Applying the divergence theorem to Eq. (14), and rearranging the terms, yields the following balance law for solvent content

$$\int_V (\dot{C} + \operatorname{div}\boldsymbol{\phi}) dV = 0. \quad (15)$$

For this equation to hold, we must have

$$\begin{aligned} \dot{C} &= -\operatorname{div}\boldsymbol{\phi} \\ \text{or } \frac{\partial C(\mathbf{X}, t)}{\partial t} + \frac{\partial \phi_j(\mathbf{X}, t)}{\partial \mathbf{X}_j} &= 0. \end{aligned} \quad (16)$$

The equation for solvent diffusion at the rate ( $\psi$ ) across the boundary at flux ( $\boldsymbol{\phi}$ ) is formulated through the law of balance law [5] given by

$$\begin{aligned} \psi &= -\boldsymbol{\phi} \cdot \mathbf{m} \\ \Rightarrow -\phi_j(\mathbf{X}, t) m_j(\mathbf{X}, t) &= \psi(\mathbf{X}, t). \end{aligned} \quad (17)$$

Multiplying Eq. (16) with an arbitrary test function  $\zeta$  and integrating with respect to volume gives

$$\int_V \frac{\partial C}{\partial t} \zeta dV + \int_V \frac{\partial \phi_j}{\partial \mathbf{X}_j} \zeta dV = 0. \quad (18)$$

Similarly, multiplying Eq. (17) with the same arbitrary test function ( $\zeta$ ), and integrating with respect to area, we get

$$-\int_S \boldsymbol{\phi}_j \mathbf{m}_j \zeta dA = \int_S \psi \zeta dA. \quad (19)$$

Applying divergence theorem on Eq. (18), putting Eq. (19) in the resultant, and on simplification we get

$$\int_V \frac{\partial C}{\partial t} \zeta dV = \int_V \boldsymbol{\phi}_j \frac{\partial \zeta}{\partial \mathbf{X}_j} dV + \int_S \psi \zeta dA. \quad (20)$$

Chemical potential gradient is required to induce swelling in the polymer. Solvent molecules in dilute phase have higher chemical potential than those in concentrated phase. This difference in potential causes solvent flow from solution to polymer. Chemical potential ( $\mu$ ) is characterized by the energy flow ( $\Theta$ ) due to solvent transport across the boundary as discussed by Gurtin et al. [16], and is given by

$$\begin{aligned} \Theta &= - \int_S \boldsymbol{\mu} \boldsymbol{\phi} \cdot \mathbf{m} dA \\ \Rightarrow \Theta &= - \int_S \boldsymbol{\mu} \psi dA. \end{aligned} \quad (21)$$

### 3.4 Free energy of the system

Free energy density is a function of concentration and deformation gradient. For an element of volume  $dV$ , Helmholtz free energy of the swelling elastomer in the current configuration is denoted by  $WdV$ . When equilibrium is attained between the fluid and the swollen elastomer, chemical potential becomes homogenous both inside the elastomer and in the surrounding solvent. Small changes  $\delta C$  in the fluid concentration and  $\delta \mathbf{F}$  in the deformation gradient of the elastomer causes changes in the free-energy density  $\delta W$ .

$$\delta W = \frac{\partial W(\mathbf{F}, C)}{\partial \mathbf{F}} \delta \mathbf{F} + \frac{\partial W(\mathbf{F}, C)}{\partial C} \delta C. \quad (22)$$

At equilibrium, free energy of the system is the amount of work done by all the loads and due to solvent transport. For small changes, rate of change of free energy of the system ( $\Lambda$ ) is given by

$$\frac{\delta \Lambda}{\delta t} = \int_V \frac{\delta W}{\delta t} dV - \int_V \mathbf{b} \frac{\delta x}{\delta t} dV - \int_S \mathbf{t} \frac{\delta x}{\delta t} dA - \int_S \boldsymbol{\mu} \psi dA. \quad (23)$$

Replacing test function with  $(\delta \mathbf{x} / \delta t)$  in Eq. (13), we get

$$\int_V \mathbf{b} \frac{\delta x}{\delta t} dV + \int_S \mathbf{t} \frac{\delta x}{\delta t} dA = \int_V \mathbf{s} \frac{\partial}{\partial \mathbf{X}} \left( \frac{\delta \mathbf{x}}{\delta t} \right) dV = \int_V \mathbf{s} \left( \frac{\delta \mathbf{F}}{\delta t} \right) dV. \quad (24)$$

Dividing Eq. (22) by  $\delta t$  and placing in Eq. (20), we get the following equation:

$$\frac{\delta W}{\delta t} = \frac{\partial W}{\partial \mathbf{F}} \left( \frac{\delta \mathbf{F}}{\delta t} \right) + \frac{\partial W}{\partial C} \left( \int_V \boldsymbol{\phi} \frac{\partial}{\partial \mathbf{X}} dV + \int_S \psi dA \right). \quad (25)$$

Substituting Eqs. (24) and (25) in Eq. (23) and rearranging the terms, we get

$$\frac{\delta \Lambda}{\delta t} = \int_V \left( \frac{\partial W}{\partial \mathbf{F}} - \mathbf{s} \right) \frac{\delta \mathbf{F}}{\delta t} dV + \int_S \left( \frac{\partial W}{\partial C} - \mu \right) \psi dA + \int_V \boldsymbol{\phi} \frac{\partial}{\partial \mathbf{X}} \left( \frac{\partial W}{\partial C} \right) dV. \quad (26)$$

According to Clausius-Duhem inequality [17], free energy of a system that is thermodynamically consistent should always decrease or be equal to zero ( $\delta \Lambda / \delta t \leq 0$ ). This condition must apply to any random value of  $\boldsymbol{\phi}$ ,  $\psi$  and  $(\delta \mathbf{x} / \delta t)$ . Accordingly, all of the above terms should be less than or equal to zero. Short-range motion is much faster than long-range transport of the solvent. Relocations occurring locally in short-range motion are assumed to be instantaneous, hence first integrand in Eq. (26) should be zero. This gives

$$\mathbf{s}_{ij} = \frac{\partial W(\mathbf{F}, C)}{\partial \mathbf{F}_{ij}}. \quad (27)$$

When equilibrium in the elastomer is reached between fluid transport and mechanical loads, chemical potential becomes uniform. This can be achieved by equating the second integrand of Eq. (26) to zero, giving the following relation

$$\mu = \frac{\partial W(\mathbf{F}, C)}{\partial C}. \quad (28)$$

When free energy density  $W(\mathbf{F}, C)$  for a system is known, and assumption of local equilibrium is applied, (27) and (28) become the equations of state for the system. At equilibrium, stress ( $\mathbf{s}_{ij}$ ) is a derivative of free-energy function with respect to deformation gradient, and chemical potential ( $\mu$ ) is defined as a derivative of free-energy with respect to concentration. Extended motion of polymer when volume change occurs due to fluid transport can be explained through kinetics, laying the foundation to develop an expression for flux due to gradient of chemical potential.

### 3.5 Kinematic constraint for network incompressibility

As explained earlier, elastomeric materials have larger values of bulk modulus as compared to shear modulus. They can therefore be considered as almost incompressible. Fluid transporting through the elastomer is assumed to be incompressible as well. Hence, overall response of swollen elastomer can be considered as incompressible. Jacobian can be defined as [6]:

$$J = \begin{bmatrix} \lambda_1 & & \\ & \lambda_2 & \\ & & \lambda_3 \end{bmatrix} \quad (29)$$

$$J \equiv \det(\mathbf{F}) = \lambda_1 \lambda_2 \lambda_3 = \frac{V_S}{V_o}.$$

Stretch is the ratio of initial and final linear dimensions that change due to deformation ( $\lambda = l_f/l_0 = t_f/t_0 = h_f/h_0$ ). This definition in terms of stretches is based on invariants. Total volume is the sum of volume of dry polymer and volume of solvent molecules absorbed in the gel. Multiplying and dividing the resulting equation by number of solvent molecules, constraint for incompressibility can be determined as follows [18]:

$$\det(\mathbf{F}) = 1 + \frac{V_s}{V_o} = 1 + \frac{V_s}{N_s} \frac{N_s}{V_o},$$

where  $\det(\mathbf{F}) = 1 + vC$ . (30)

In order to embed incompressibility, an integral should be added to the free-energy density function. Using Lagrange multiplier ( $p$ ) to optimize the functions, applying the constraint [5] of Eq. (30), we get

$$\kappa = \int_V p \{1 + vC - \det(\mathbf{F})\} dV. \quad (31)$$

Differentiating Eq. (31) with respect to  $\mathbf{F}$  and  $C$ , and using the identity  $\partial \det(\mathbf{F}) / \partial \mathbf{F} = \mathbf{F}^{-T} \det(\mathbf{F})$  [14], equations of state can be rewritten as follows:

$$\frac{\partial \kappa}{\partial \mathbf{F}} = -p \mathbf{F}^{-T} \det(\mathbf{F})$$

$$\frac{\partial \kappa}{\partial C} = pv. \quad (32)$$

Stress and chemical potential can now be defined as

$$\mathbf{s} = \frac{\partial W(\mathbf{F}, C)}{\partial \mathbf{F}} - p \mathbf{F}^{-T} \det(\mathbf{F})$$

(33)

and  $\mu = \frac{\partial W(\mathbf{F}, C)}{\partial C} + pv.$

### 3.6 Kinetics

The only driving force causing swelling of the elastomer is the amount of fluid transport into the network, resulting in swelling and stretching of networks. This is the reason that kinetics needs to describe the fluid motion in terms of flux and gradient of chemical potential. Some authors consider gel as poro-elastic or porous and use Darcy's law to model the amount of fluid influx [10, 19]. In porous media, a body is considered to be made up of pores such that permeability is related to the square of pore size. But in a swollen elastomer, major portion of the body is comprised of solvent and when load is applied on it, maximum resistance comes from the solvent molecules as in diffusion. Kinetic theory has also been developed by Tanaka and Fillmore [20] by considering friction with rate-dependent swelling. This theory has limited applicability as it does not consider large deformations. Other authors define a kinetic law based on diffusion mechanism for solvent migrations in elastic material [4–6]. Mobility tensor should be dependent on deformation gradient and solvent concentration. For defining mobility tensor, we use the relations similar to Chester and Anand [10] and Hong et al. [5]:

$$\phi_k = -\mathbf{M}_{KM} \frac{\partial \mu}{\partial \mathbf{X}_M}. \quad (34)$$

Mobility tensor is positive definite and symmetric. Feynman et al. [21] derived an expression for diffusion in which flux is proportional to gradient of chemical potential. It explains the interrelationship of flux, fluid concentration, diffusion, and gradient of chemical potential in terms of true quantities:

$$\phi_i = -\frac{cD}{kT} \frac{\partial \mu}{\partial \mathbf{x}_i}. \quad (35)$$

In engineering applications, a property based on its original or initial value is termed as nominal quantity. On the other hand, true quantities are based on instantaneous properties. For example, a structural member under the influence of load deforms, resulting in reduction of cross-sectional area. In nominal stresses, the cross-sectional area is assumed constant during the deformation and stress is determined, known as nominal or engineering stress. While in true stress, force is divided by the instantaneous area. True concentration and flux can be converted to nominal values through the relationships  $c = C/\det(\mathbf{F})$  and  $\phi = \mathbf{F}\phi/\det(\mathbf{F})$ , respectively. Also, using partial derivative chain rule, we can express gradient of chemical potential as

$$\frac{\partial \mu}{\partial \mathbf{X}_M} = \frac{\partial \mu}{\partial \mathbf{x}_i} \mathbf{F}_{iM}. \quad (36)$$

Replacing true concentration and true flux in Eq. (5) by their nominal values, we get

$$\frac{\mathbf{F}_{iK}}{\det(\mathbf{F})} \phi = -\frac{C}{\det(\mathbf{F})} \frac{D}{kT} \frac{\partial \mu}{\partial \mathbf{x}_i}. \quad (37)$$

Substituting Eqs. (34) and (36), along with the incompressibility condition from Eq. (30), into Eq. (37), relation for mobility tensor can be obtained:

$$\begin{aligned} \frac{\mathbf{F}_{iK}}{\det(\mathbf{F})} \mathbf{M}_{KM} \frac{\partial \mu}{\partial \mathbf{X}_M} &= \frac{C}{\det(\mathbf{F})} \frac{D}{kT} \frac{\partial \mu}{\partial \mathbf{x}_i} \\ \Rightarrow \mathbf{M}_{KM} &= \frac{D}{vkT} \mathbf{F}_{iK}^{-T} \mathbf{F}_{iM}^{-T} \{\det(\mathbf{F}) - 1\}. \end{aligned} \quad (38)$$

### 3.7 Thermodynamics of mixing

Thermodynamics involved in polymer and solvent mixing is very important in the development of an analytical model for polymer swelling. The theoretical basis for understanding the behavior of polymer solutions was established independently by Huggins [22] and Flory [23]. Flory-Huggins theory gives the energy of mixing for a pure polymer with a pure solvent in terms of enthalpy and entropy of mixing. **Figure 4** presents the lattice model for mixing of polymer and solvent.

Statistical explanation of entropy is used to determine the number of probable positions that the polymer can attain in the solution. Before mixing, both polymer and solvent have no unique state. After mixing, many probable states can be attained, given by

$$\Omega = \frac{N!}{N_s!N_p!}. \quad (39)$$

Entropy for free energy of mixing can be specified according to Boltzmann expression as follows:

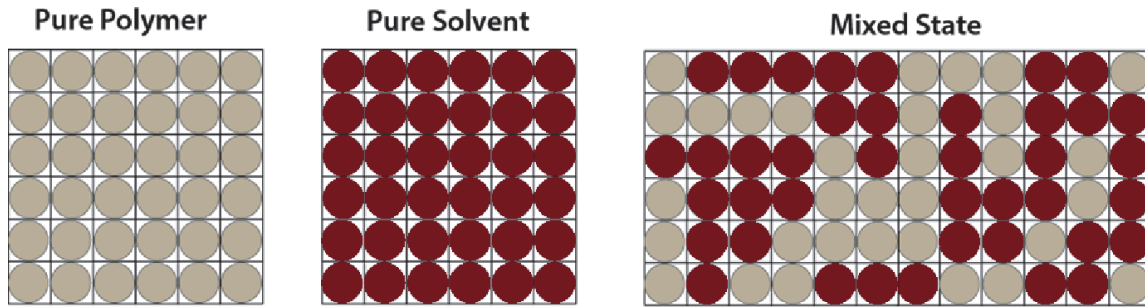


**Figure 4.**  
 Lattice model for mixing of polymer and solvent.

$$\Delta S = k \ln \Omega, \quad (40)$$

where  $k$  is the Boltzmann constant. Using logarithmic principles and Sterling's approximation, Eq. (40) can be rewritten in terms of volume fraction of polymer ( $\Phi_P$ ) and solvent ( $\Phi_S$ ) as follows:

$$\Delta S = -k(N_s \ln \Phi_S + N_P \ln \Phi_P). \quad (41)$$

Enthalpy of mixing is defined in terms of a dimensionless entity known as polymer-solvent interaction parameter ( $\chi$ ). It measures the degree of interaction between polymer and solvent as well as polymer and polymer:

$$\Delta H = \chi k T N_s \Phi_P. \quad (42)$$

For a closed system at constant pressure and temperature, Gibbs free energy can be defined as

$$\Delta G = \Delta H - T \Delta S. \quad (43)$$

Putting Eqs. (41) and (42) in Eq. (43), we get the expression

$$\Delta G = k T (N_s \ln \Phi_S + N_P \ln \Phi_P + \chi N_s \Phi_P). \quad (44)$$

Noting that ( $\Phi_S + \Phi_P = 1$ ), and using Eq. (30), we get

$$\begin{aligned} \Phi_S &= 1 - \Phi_P = 1 - \frac{1}{J} \\ \Rightarrow \Phi_S &= \frac{vC}{1 + vC}. \end{aligned} \quad (45)$$

Substituting Eqs. (45) into Eq. (44), and neglecting the middle term as it is very small compared to the remaining terms, the strain energy density function for mixing ( $W_m = \Delta G/V_o$ ) can be expressed as:

$$\begin{aligned} W_m &= \frac{kT}{V_o} \left( N_s \ln \frac{vC}{1 + vC} + \chi N_s \frac{1}{1 + vC} \right) \\ \Rightarrow W_m &= \frac{kT}{v} \left( vC \ln \frac{vC}{1 + vC} + \chi \frac{vC}{1 + vC} \right). \end{aligned} \quad (46)$$

A similar expression has also been used by Chester and Anand [10] Duda et al. [24] and Kang and Huang [6]. Equation developed by Hong et al. [5] for strain energy density of mixing is different by only a constant value as compared to the

above expression, which is negligible in deformation due to swelling. Flory and Rehner [25] postulated that for gels, free energy density is a combination of strain energy density function due to thermodynamics of mixing and stretching of polymer networks:

$$W(\mathbf{F}, C) = W_m(C) + W_S(\mathbf{F}). \quad (47)$$

Strain energy density function for stretching deformation can be based on either Gaussian or non-Gaussian theory. As described earlier, Gaussian theory mainly deals with the scenarios where short stretching of polymer chains is considered, so these models work well only for small deformations and are unable to match the deformation patterns at large strains. Most of the swelling models currently available use Gaussian statistics [8], and are therefore unable to give reasonable predictions for large swelling. Proposed analytical model is based on non-Gaussian theory, while Ogden strain energy function [9] is used to account for the limited extensibility. Ogden model is given by the following relation in terms of principal stretches:

$$W_S = \sum_{n=1}^Q \frac{\mu_n}{\alpha_n} (\lambda_1^{\alpha_n} + \lambda_2^{\alpha_n} + \lambda_3^{\alpha_n} - 3). \quad (48)$$

Here,  $\mu_n$  and  $\alpha_n$  are material constants that are determined by fitting the experimental data, and  $Q$  is a positive definite integer. These material constants are related to shear modulus ( $G$ ):

$$\sum_{n=1}^Q \mu_n \alpha_n = 2G. \quad (49)$$

For the proposed model, second degree Ogden strain energy function is used as it gives the closest prediction (as explained in Chapter 6). Expand Eq. (48) for second degree, and simplifying, we get the following relation:

$$\begin{aligned} W_S &= \frac{\mu_1}{\alpha_1} (\lambda_1^{\alpha_1} + \lambda_2^{\alpha_1} + \lambda_3^{\alpha_1} - 3) + \frac{\mu_2}{\alpha_2} (\lambda_1^{\alpha_2} + \lambda_2^{\alpha_2} + \lambda_3^{\alpha_2} - 3) \\ &\Rightarrow \mu_1 \alpha_1 + \mu_2 \alpha_2 = 2G. \end{aligned} \quad (50)$$

Putting Eqs. (46) and (50) into (47), we get the following strain energy density function:

$$\begin{aligned} W(\mathbf{F}, C) &= \frac{\mu_1}{\alpha_1} (\lambda_1^{\alpha_1} + \lambda_2^{\alpha_1} + \lambda_3^{\alpha_1} - 3) + \frac{\mu_2}{\alpha_2} (\lambda_1^{\alpha_2} + \lambda_2^{\alpha_2} + \lambda_3^{\alpha_2} - 3) \\ &\quad + \frac{kT}{v} \left( vC \ln \frac{vC}{1+vC} + \chi \frac{vC}{1+vC} \right) \end{aligned} \quad (51)$$

Knowing that deformation gradient can be represented as  $\mathbf{F} = \lambda \mathbf{I}$  [13, 7], and differentiating Eq. (51) with respect to  $\lambda$ , we get

$$\frac{\partial W}{\partial \mathbf{F}} = \frac{\partial W}{\partial \lambda_i} = \mu_1 \lambda_i^{\alpha_1 - 1} + \mu_2 \lambda_i^{\alpha_2 - 1}. \quad (52)$$

Differentiation of Eq. (50) with respect to fluid concentration results in the following expression:

$$\frac{\partial W}{\partial C} = kT \left[ \ln \frac{vC}{1+vC} + \frac{1}{1+vC} + \chi \frac{1}{(1+vC)^2} \right]. \quad (53)$$

Substituting the expressions for  $\partial W/\partial F$  from Eq. (52), and  $\partial W/\partial C$  from Eq. (53), into Eq. (33), and using (29), equations of state can be converted into the following form:

$$\mathbf{s}_i = \mu_1 \lambda_i^{\alpha_1 - 1} + \mu_2 \lambda_i^{\alpha_2 - 1} - p \lambda_i^{-1} \lambda_1 \lambda_2 \lambda_3$$

and 
$$\mu = kT \left[ \ln \frac{vC}{1+vC} + \frac{1}{1+vC} + \chi \frac{1}{(1+vC)^2} \right] + pv. \quad (54)$$

Eq. (54) can be expanded for the three nominal stresses as follows:

$$\begin{aligned} \mathbf{s}_1 &= \mu_1 \lambda_1^{\alpha_1 - 1} + \mu_2 \lambda_1^{\alpha_2 - 1} - p \lambda_2 \lambda_3 \\ \mathbf{s}_2 &= \mu_1 \lambda_2^{\alpha_1 - 1} + \mu_2 \lambda_2^{\alpha_2 - 1} - p \lambda_1 \lambda_3 \\ \mathbf{s}_3 &= \mu_1 \lambda_3^{\alpha_1 - 1} + \mu_2 \lambda_3^{\alpha_2 - 1} - p \lambda_1 \lambda_2. \end{aligned} \quad (55)$$

On the other hand, the two equations in (54) can be combined to obtain a constitutive relationship for modeling of swelling phenomenon:

$$\mathbf{s}_i = \mu_1 \lambda_i^{\alpha_1 - 1} + \mu_2 \lambda_i^{\alpha_2 - 1} - \frac{\lambda_i^{-1} \lambda_1 \lambda_2 \lambda_3}{v} \left[ \mu - kT \left\{ \ln \frac{vC}{1+vC} + \frac{1}{1+vC} + \chi \frac{1}{(1+vC)^2} \right\} \right] \quad (56)$$

Eq. (56) provides a non-linear model for the phenomenon of swelling in elastomeric materials, considering non-Gaussian theory of polymer network stretching. This model takes mechanical as well as solvent properties as input, along with environmental conditions such as temperature, water salinity, swelling medium's coefficient of diffusion, polymer-solvent interaction parameter, etc.

In order to solve the equations of state, a case of free equilibrium swelling is considered. It is assumed that when dry elastomer is immersed in a solvent, it swells, and equilibrium is achieved after some time. At equilibrium between elastomer and diffusing solvent, chemical potential is negligible. Swelling is considered to be homogenous throughout the elastomer, making stretches equal in all directions. Replacing principal stretches with equivalent swelling stretch ( $\lambda_S$ ), and setting up chemical potential equal to zero in Eq. (56), we get

$$\mathbf{s}_i = \mu_1 \lambda_S^{\alpha_1 - 1} + \mu_2 \lambda_S^{\alpha_2 - 1} + \frac{\lambda_S^2}{v} kT \left[ \ln \frac{vC}{1+vC} + \frac{1}{1+vC} + \chi \frac{1}{(1+vC)^2} \right]. \quad (57)$$

Using the identity of Eq. (30), we can write  $1+vC = \lambda_S^3$  and  $vC = \lambda_S^3 - 1$ . Replacing in Eq. (57), and simplifying,

$$\mathbf{s}_i = \mu_1 \lambda_S^{\alpha_1 - 1} + \mu_2 \lambda_S^{\alpha_2 - 1} + \frac{\lambda_S^2}{v} kT \left[ \ln \left( 1 - \frac{1}{\lambda_S^3} \right) + \frac{1}{\lambda_S^3} + \chi \frac{1}{\lambda_S^6} \right]. \quad (58)$$

The elastomer is considered to be under no constraint. Application of this no-constraint condition on the elastomer results in no stress. Hence Eq. (58) can be transformed by embedding stress value equals to zero:

$$\mu_1 \lambda_S^{\alpha_1 - 3} + \mu_2 \lambda_S^{\alpha_2 - 3} + \frac{kT}{v} \left[ \ln \left( 1 - \frac{1}{\lambda_S^3} \right) + \frac{1}{\lambda_S^3} + \chi \frac{1}{\lambda_S^6} \right] = 0. \quad (59)$$

## 4. Model validation

Validation of the model developed above requires the comparison of model predictions against experimental results. For this purpose, a series of experiments were performed under specific conditions. Some experimental results are used as input to the model (for evaluation of parameters), while other results are used for model validation. Logical flow of activities for model validation is shown in **Figure 5**. Swelling related experiments are discussed in detail in Chapters 3 and 7. Experimental work required to determine diffusion coefficients and the polymer-solvent interaction parameter and is explained below.

### 4.1 Experimental investigation

Experiments were conducted (already described in Chapter 7) on disc samples of two different water swelling elastomers, in salt solutions of low and high salinities (0.6% and 12%), at room temperature and 50°C. During the one-month swelling period, readings (volume, thickness, mass, and hardness) were taken before swelling and after 1, 2, 4, 7, 10, 16, 23, and 30 days of swelling. Stress-strain relations from compression and bulk tests were used to determine values of bulk modulus, and different structural properties. Evaluation of other solvent and polymer properties (diffusion coefficient, polymer-solvent interaction parameter, and molar volume of swelling solvent) is discussed below.

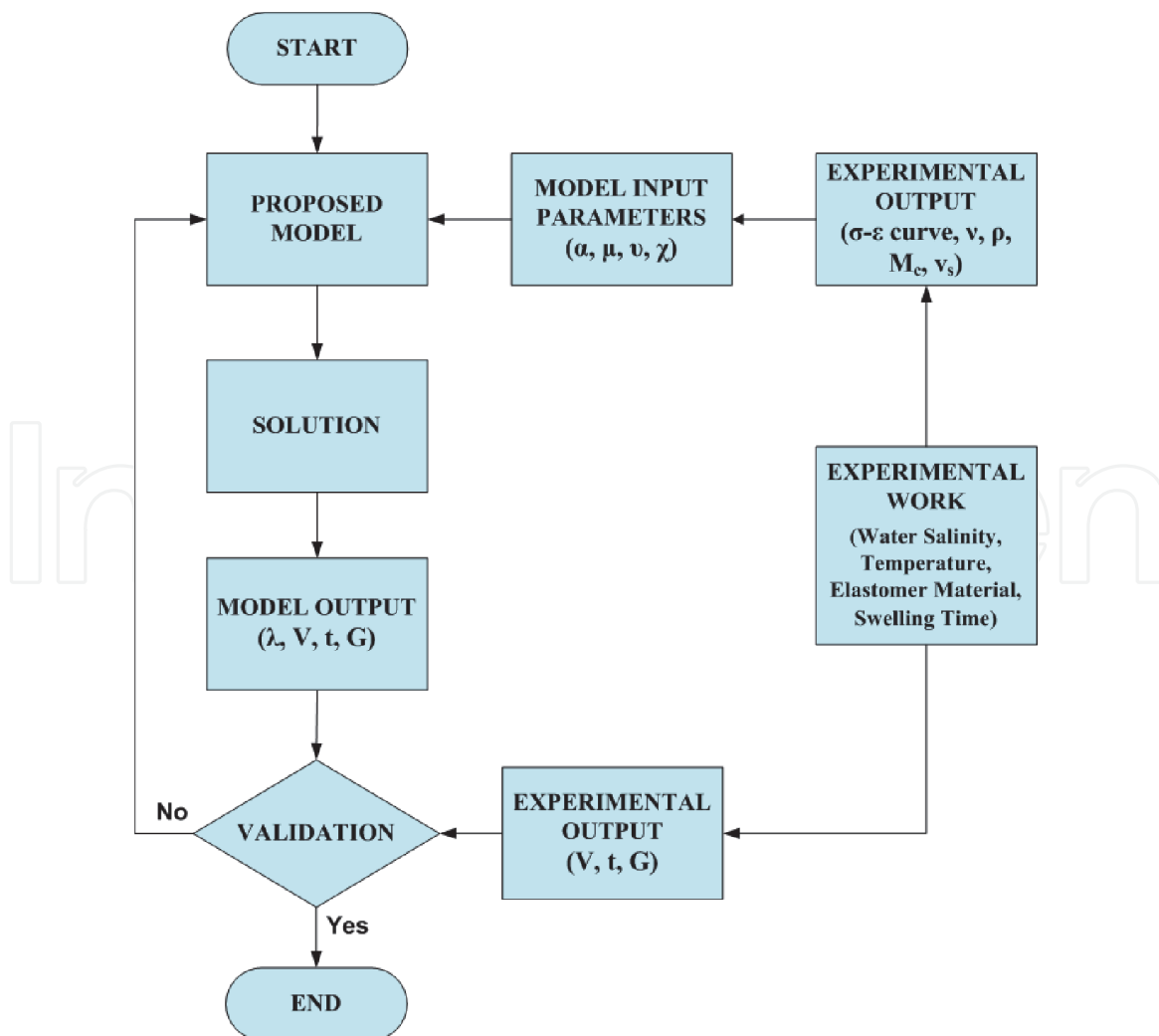


**Figure 5.**  
Flow diagram of activities required for model validation.

#### 4.1.1 Diffusion coefficient

When a dry polymer is immersed into water of a specific salinity, solvent starts diffusing into the polymer due to chemical potential gradient. Diffusion coefficients for low and high salinity solutions should be known in order to correctly predict the amount of swelling. Stokes-Einstein formula [26] is used here to evaluate the diffusion coefficients for low and high salinity solutions.

For a fluid with no flow separation, the drag force is given by

$$F_D = \frac{24 \left( \frac{\rho v^2}{2} \right) A}{Re}. \quad (60)$$

We know that Reynold's number and cross-sectional area are given by  $Re = Dv\rho/\eta$  and  $A = \pi D^2/4$  respectively. Therefore,

$$F_D = 6\pi R\eta v. \quad (61)$$

It is known that drag force can also be represented as

$$F_D = \zeta v, \quad (62)$$

where  $\zeta$  is Stoke's friction factor, and can be written as

$$\zeta = 6\pi R\eta. \quad (63)$$

The diffusion coefficient ( $D$ ) is given by Einstein's equation as

$$D = \frac{kT}{\zeta}. \quad (64)$$

Using Stoke's friction factor, this becomes

$$D = \frac{kT}{6\pi R\eta}. \quad (65)$$

Here,  $k$  is the Boltzmann constant,  $T$  is the absolute temperature,  $R$  is the radius of solvent particle, and  $\eta$  is the viscosity.

In order to determine diffusion coefficient, viscosity and density of water at low and high salinities are required for all test conditions. To determine the viscosity, Cannon-Fenske [27] apparatus (**Figure 6**) of size 50 is used. Liquid (whose viscosity is to be determined) is filled in the apparatus slightly above the top-bulb. Fluid is then allowed to flow downwards, pass through the tube, and collect at the bigger bulb at the bottom. Time is recorded for fluid to cross two marks at the top and bottom of the second bulb. Readings are taken at the same temperature at which all swelling related experiments are conducted.

Density of elastomer samples is calculated by determining their mass and volume after each swelling period, for both salinities and at both temperatures. Mass of the elastomer is increased by inflow of salt water into the material. At the same time, volume is increased through swelling. As both mass and volume increase almost proportionally, density does not change too much. Calculated density values are  $0.967 \text{ g/cm}^3$  and  $1.016 \text{ g/cm}^3$  for low salinity water at room temperature and  $50^\circ\text{C}$ , and  $1.05 \text{ g/cm}^3$  and  $1.0898 \text{ g/cm}^3$  for high salinity water at the two temperatures respectively.



**Figure 6.**  
Cannon-Fenske apparatus used for viscosity measurement.

Mean time for low and high salinity water to pass from the first to the second mark in Cannon-Fenske apparatus was recorded as 157 and 170 sec for 50°C, and 219 and 260 sec at room temperature, respectively. Multiplying by the apparatus factor of 0.004, we get viscosity (centistokes) values of 0.628 and 0.68 at 50°C, and 0.876 and 0.1.04 at room temperature, for low and high salinities respectively. Multiplying this dynamic viscosity with density yields the kinematic viscosity in Pascal-second units. Substituting these values into Eq. (65) gives the required value of diffusion coefficient for each condition. These experimentally determined values of viscosity and diffusion coefficient are summarized in **Table 1**.

It can be seen that the diffusion coefficient has higher value in low salinity water as compared to high salinity water, for both room and 50°C temperatures. This higher diffusion amount causes faster swelling rate when the elastomer is kept in low salinity solutions. For same salinity, diffusion coefficient has higher values for

Viscosity (Pa-s x10 <sup>-3</sup> )		Temperature	
		Low (room)	High (50 °C)
Salinity	Low (0.6%)	0.89	0.607
	High (12%)	1.1334	0.714
Diffusion coefficient(m <sup>2</sup> /s x10 <sup>-10</sup> )		Temperature	
		Low (room)	High (50 °C)
Salinity	Low (0.6%)	8.22	11.65
	High (12%)	6.46	9.9

**Table 1.**  
Viscosity and diffusion coefficient at two salinities and two temperatures.

higher temperatures, again matching the observed trend for higher amount of elastomer swelling at higher temperature.

Though the mechanism of swelling has been discussed earlier (Chapters 3 and 7), let us revisit the issue in the context of diffusion. When sodium chloride dissolves in water, crystalline structure of sodium and chlorine transform into positive and negative ions surrounded by water molecules. Water molecules close to the ions have strong attraction. When polymer is exposed to brine solution, water molecules diffuse into the empty spaces and begin to fill the voids, resulting in swelling. Ions surrounded by water molecules also enter the polymer but somewhat slowly due to stronger attraction. Ultimately, the polymer is filled by water molecules and ions. Low salinity solution has less number of ions, hence water fills the spaces more quickly as compared to high salinity solution. That is why diffusion takes place at a slower rate in high salinity salt solution.

#### 4.1.2 Polymer-solvent interaction parameter

Polymer-solvent interaction parameter ( $\chi$ ), also known as Flory-Huggins interaction parameter, is an important dimensionless temperature-based property of a polymer which controls the amount of swelling. If  $\chi$  increases, liquid seepage takes place leading to de-swelling or contraction of the elastomer. A decrease in  $\chi$ -value leads to swelling of the elastomer (volume increase). Different experimental studies are available in published literature which discuss methods of determining  $\chi$ . Orwoll and Arnold [28] use inverse gas chromatography. Papageorgiou et al. [29] apply differential scanning calorimetry. Silva et al. [30] use measurement of melting temperature of the polymer blend. Clarke et al. [31] use micelle spacings with secondary ion mass spectroscopy, contact angle of blend droplet, and neutron reflectometry. In all experimental methods, the polymer needs to dissociate in order to determine  $\chi$  for a particular polymer-solvent mixture. Both elastomer materials used in swelling experiments were found to be insoluble in all solvents available (polar as well non-polar solvents). An in-depth search was carried out to find a method for determination of  $\chi$  that does not require elastomer dissociation. Treloar [8] gives a relationship between molecular mass and volume swelling ratio, density of polymer, molar volume of swelling liquid, and polymer-solvent interaction parameter:

$$\begin{aligned} \frac{\rho V_1}{M_c} \left( v_s^{1/3} - \frac{v}{2} \right) + [ \ln(1 - v_s) + v_s + \chi v_s^2 ] &= 0 \\ \Rightarrow \chi &= -\frac{1}{v_s^2} \left[ \frac{\rho V_1}{M_c} \left( v_s^{1/3} - \frac{v_s}{2} \right) + \ln(1 - v_s) + v_s \right]. \end{aligned} \quad (66)$$

The above Eq. (66) is used in this work to determine the value of  $\chi$  for each data set. Molecular mass ( $M_c$ ) is already determined using experiments described in Chapter 7. This unique method for the determination of the interaction parameter ( $\chi$ ), using mechanical and structural properties of a polymer, has not been used in any of the published works. Molar volume ( $V_1$ ) of water is  $0.00018 \text{ m}^3$ . Values of density of elastomer after different swelling periods are given above. **Table 2** lists the experimentally determined values of volume swelling ratio ( $v_s$ ), which is the ratio of initial to swelled volume.

**Figure 7** shows the variation of  $\chi$  against swelling time (days) for both materials in low and high salinity brine. For all the cases,  $\chi$  values tend to decrease with swelling time, following the default trend [13]. It can also be seen that  $\chi$  values drop more in low salinity brine, in line with the earlier observation that these elastomers swell more in brines of lower concentration. Initially faster and then more gradual

Days of Swelling	Volume Swelling Ratio ( $v_s$ )			
	Material-A		Material-B	
	Low-Salinity	High-Salinity	Low-Salinity	High-Salinity
1	0.455	0.543	0.494	0.646
3	0.392	0.505	0.403	0.525
6	0.323	0.465	0.318	0.474
9	0.291	0.431	0.292	0.442
15	0.245	0.365	0.264	0.438
22	0.234	0.347	0.249	0.389
30	0.234	0.338	0.232	0.376

**Table 2.**  
Volume swelling ratio for materials A and B.

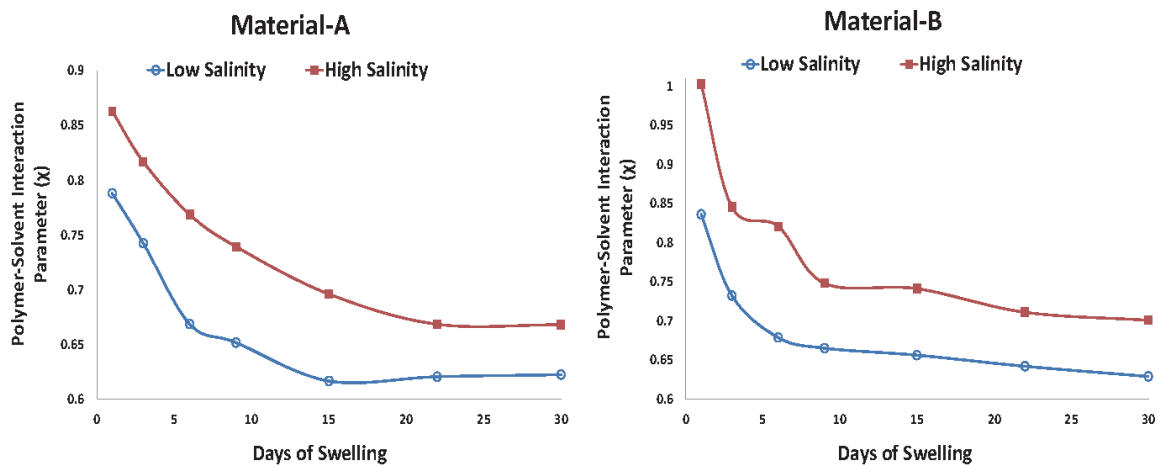


**Figure 7.**  
Variation of polymer-solvent interaction parameter ( $\chi$ ) against swelling time; materials A and B; low and high salinity.

decrease in  $\chi$  also matches the behavior of these quick-swelling elastomers. Slight fluctuation of  $\chi$  variation for material-B is also consistent with earlier observations about swelling behavior.

## 4.2 Computational code

For the solution of the final Eq. (59) of the developed model, and to extract different values required for analysis, a MATLAB code is written. This requires inputs such as material coefficients, temperature, volume per solvent molecule, interaction parameter, etc. Logical sequence of different steps involved are shown in **Figure 8**. Using all the input values, and going through the various steps of the iterative scheme, the code estimates the magnitudes of swelling stretches after each swelling period (days) and for each material and each salinity (low and high). Comparison of different outcomes of the model with experimental results is discussed in next section.

## 5. Analysis of results

New model starts with Ogden-2 as its basis, but is changed into a totally new relationship (Eq. 59) by the introduction of terms for diffusion and

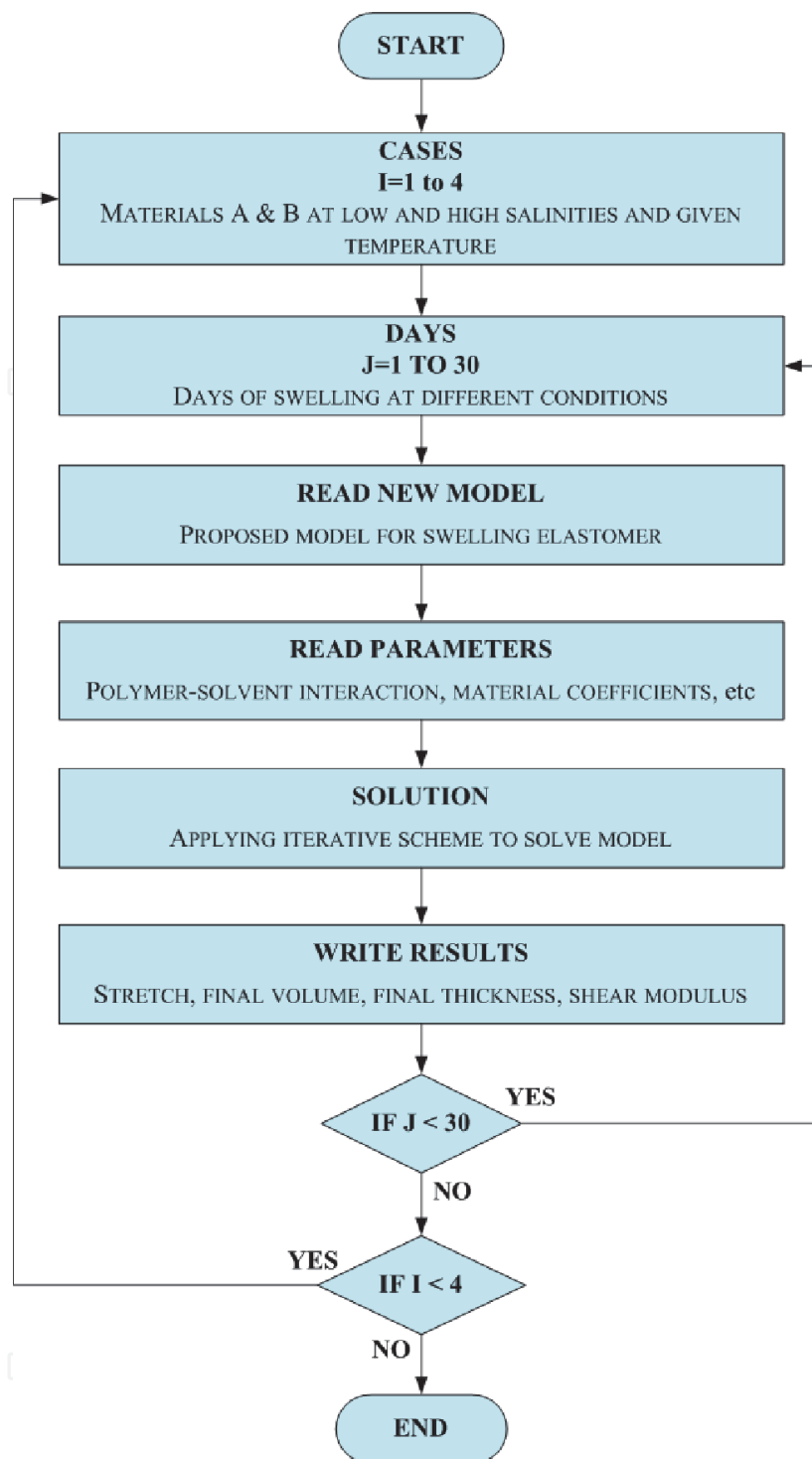


**Figure 8.**  
 Logical sequence of steps involved in the MATLAB code.

thermodynamics of mixing. Material coefficients for Ogden model ( $\mu_1, \mu_{12}, \alpha_1, \alpha_2$ ) are determined from experimental stress–strain curves and Poisson’s ratio ( $\nu$ ). Polymer-solvent interaction parameter ( $\chi$ ) is determined from mechanical, structural, and chemical properties: density ( $\rho$ ) and chain molecular mass ( $M_c$ ) of the elastomer, molar volume of water ( $V_1$ ), and volume swelling ratio ( $\nu_s$ ). Other input parameters needed are temperature ( $T$ ), Boltzmann constant ( $k$ ), and swelled volume per solvent molecule ( $v$ ). Through an iterative solution, major output from the new model is the value of swelling stretch ( $\lambda$ ) at each stage of swelling, from which the amount of volume and thickness change and the shear modulus ( $G$ ) are calculated.

### 5.1 Elastomer stretch

**Figure 9** gives the variation of stretch for materials *A* and *B* under both salinities. Results show an increase in stretch throughout the swelling period for both the materials, sharply in the beginning, then more slowly. This result is in good agreement with the fact that swelling leads to volume increase, which is represented by an increase in the stretch value. Higher stretch values are observed in low salinity solvent, in line with the actual behavior of swelling elastomers which swell more in low salinity due to higher chemical potential gradient and higher diffusion coefficient. Minor fluctuations in the variation of amount of stretch are also similar to the fluctuations in volume and thickness swelling reported and analyzed in Chapters 3 and 7.

### 5.2 Volume swelling

Volume after swelling can be calculated from the amount of stretch determined from the model:

$$V_{Model} = \lambda_S^3 * V_o. \tag{67}$$

**Figures 10** and **11** show the comparison between experimental and model-predicted volume at various stages of swelling for materials *A* and *B* under the two

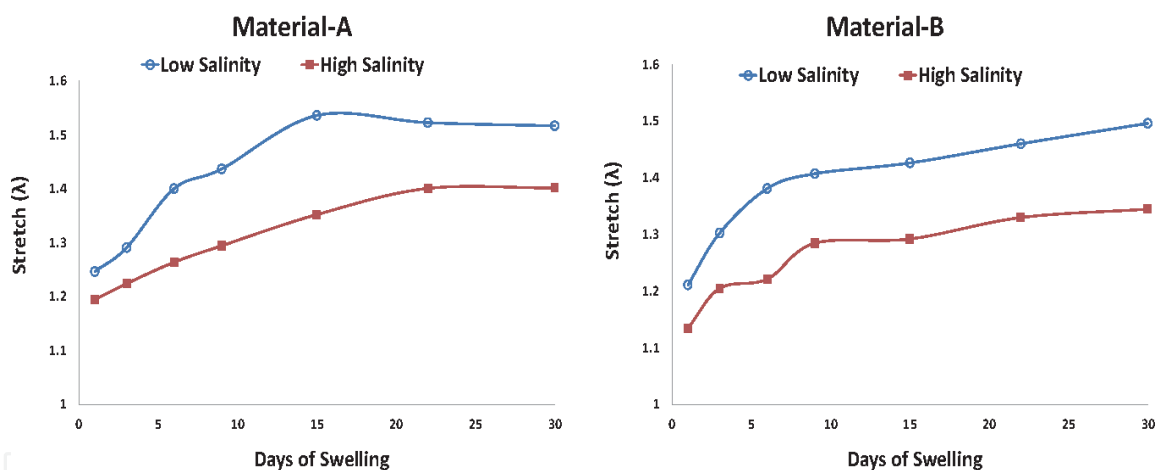


**Figure 9.** Amount of stretch vs. swelling time for materials *A* and *B*; both salinities.

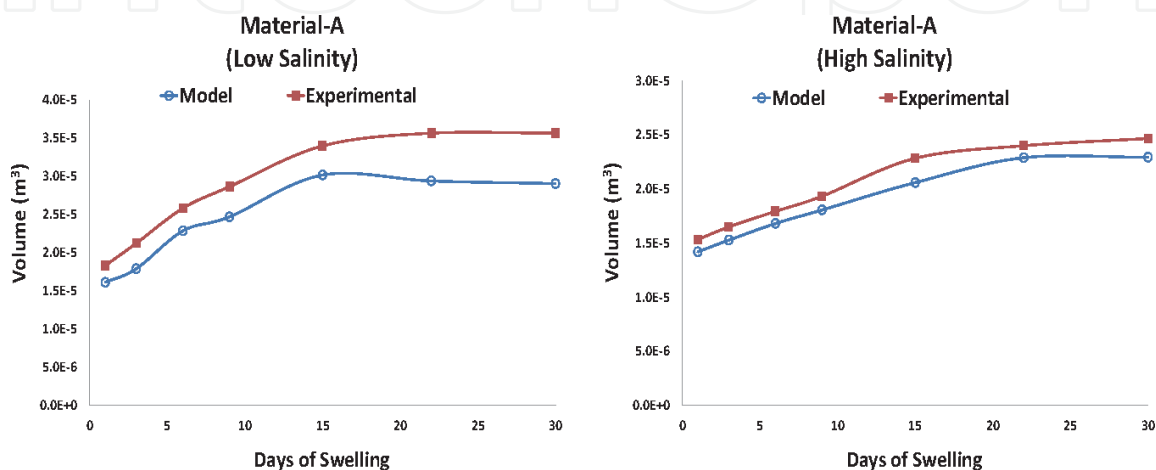


**Figure 10.** Model-predicted and experimental results for volume swelling; material-*A*; both salinities.

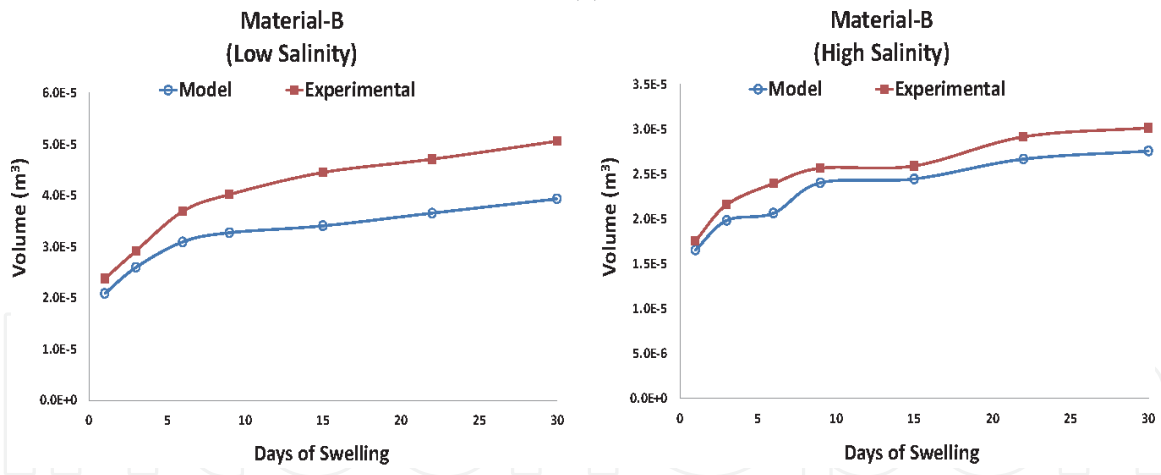


**Figure 11.** Model-predicted and experimental results for volume swelling; material-B; both salinities.

salinities. Following the pattern of experimental results, predicted amount of elastomer volume increases with swelling time (days). Slight fluctuations in volume swelling are also in line with experimental results, and due to reasons explained earlier. There is a small difference between experimental and model results, the model consistently underestimating the value of volume swelling. This underestimation gives a more conservative estimate of swelling amount, which is better and safer in terms of seal design and development.

### 5.3 Thickness swelling

Final thickness after each swelling stage can be calculated using swelling stretch as follows:

$$t_{Model} = \lambda_S * t_o. \quad (68)$$

Comparison between experimental and predicted values of thickness at various stages of swelling is shown in **Figures 12** and **13** for materials A and B in both salinities. There is a gradual increase in the amount of thickness with more days of swelling, with a reasonably good agreement between predicted values and experimental results. As observed earlier, there is more thickness swelling under lower salinity brine.

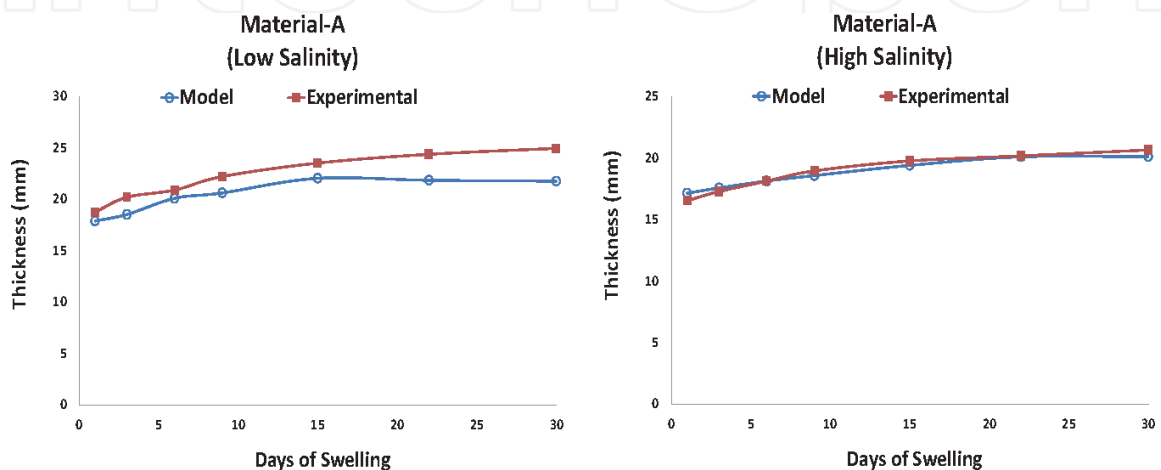


**Figure 12.** Model-predicted and experimental results for thickness swelling; material-A; both salinities.

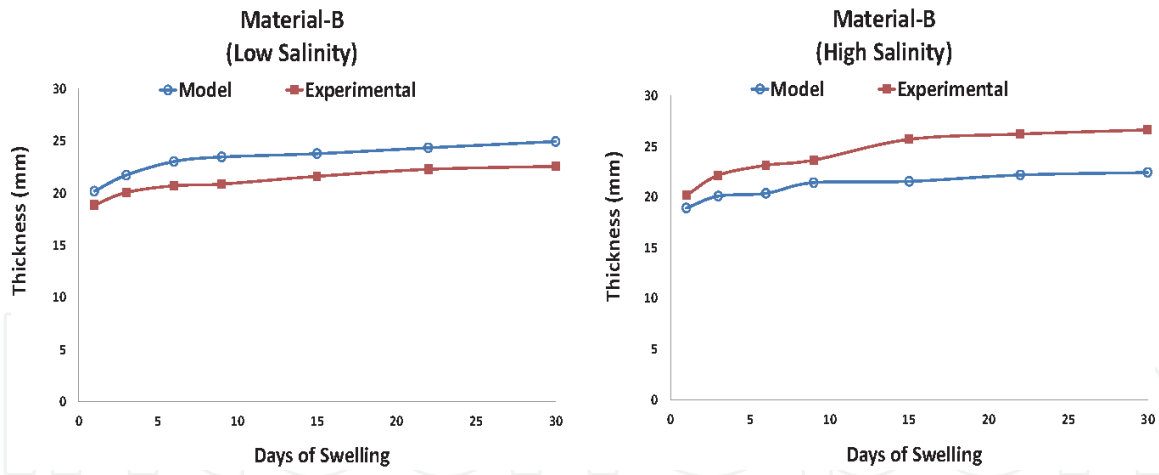


**Figure 13.** Model-predicted and experimental results for thickness swelling; material-B; both salinities.

## 5.4 Shear modulus

Amount of stretch predicted from the model can be used to determine the value of shear modulus using the following relationship:

$$G_{Model} = - \frac{N_c v (\mu_1 \lambda_S^{\alpha_1 - 3} + \mu_2 \lambda_S^{\alpha_2 - 3})}{\left[ \ln \left( 1 - \frac{1}{\lambda_S^3} \right) + \frac{1}{\lambda_S^3} + \chi \frac{1}{\lambda_S^6} \right]}. \quad (69)$$

Predicted and experimental values of shear modulus are plotted against swelling time in **Figures 14** and **15** for the two materials and salinities. For further comparison, variation of shear modulus through numerical simulation (Chapter 7) using the best available hyperelastic material model (Ogden-2) is also shown. *It is reassuring to observe that there is a very good agreement between values predicted by the new model and experimental results, even in portions where there are major fluctuations. Also, predictions from the new model are much closer than numerical simulations using the best hyperelastic material model.* Even though hyperelastic material models are based on the theory of shear, simulated values of  $G$  using the current best model (Ogden-2) show notable variations from the experimental values. As discussed at the end of Chapter 6, hyperelastic models can be used to predict the behavior of swelling elastomers only as a last resort, with some errors.

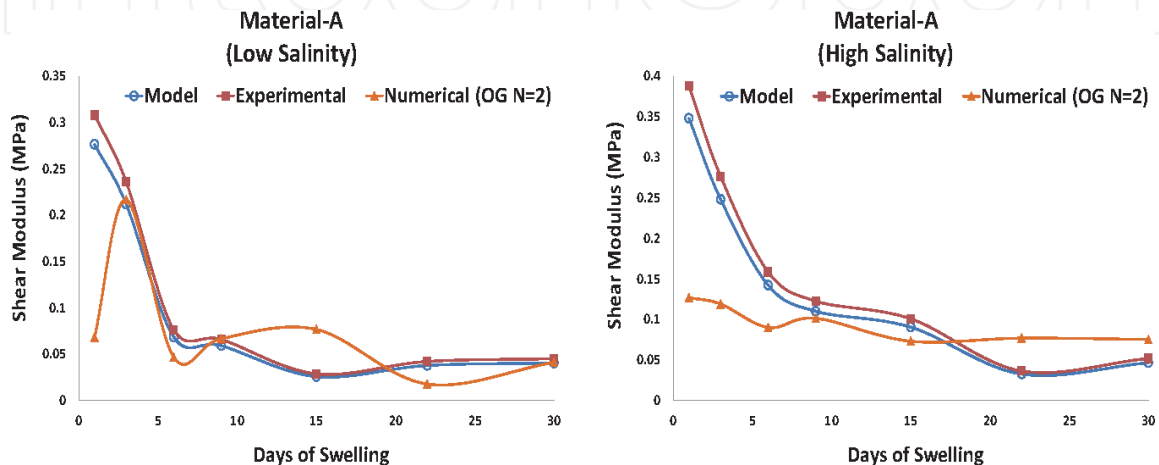


**Figure 14.** Variation of shear modulus against swelling time from new model, experiments, and FE simulation (Ogden-2); material-A; both salinities.

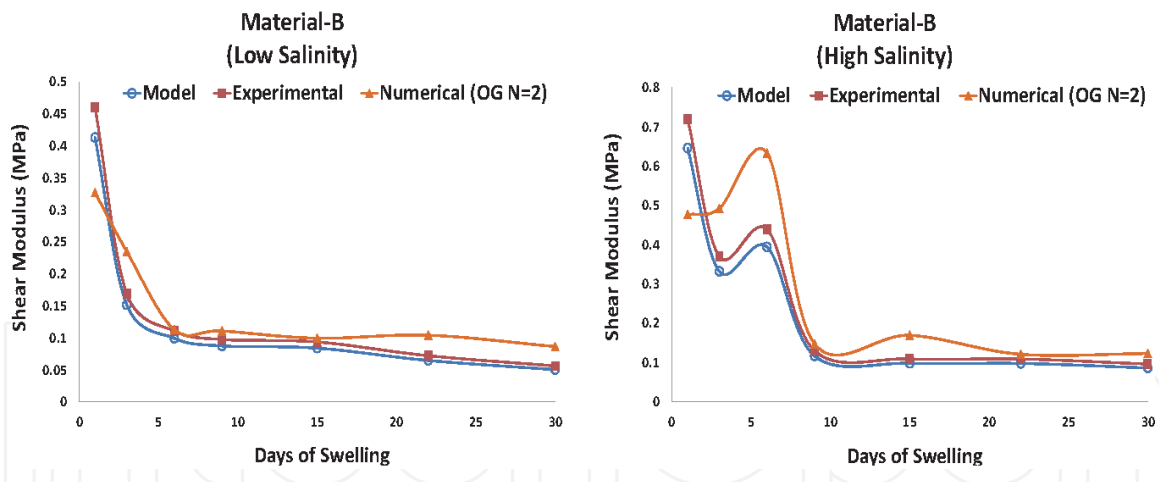


**Figure 15.** Variation of shear modulus against swelling time from new model, experiments, and FE simulation (Ogden-2); material-B; both salinities.

This is mainly because these models do not include the effect of diffusion and thermodynamics of mixing. As the new model includes all these effects, its predictions are much closer to the actual values.

This new model is not material-specific, and can be applied to any situation where swelling is taking place. As the use of swelling elastomers in the petroleum industry is a major category of such applications, these results are used here to validate the model predictions. However, the same model can be used to predict the behavior of other soft materials under swelling such as tissue, cartilage, and other biological materials.

## 6. Conclusions

A new analytical model has been developed for predicting the behavior of swelling elastomers, based on nonlinear and non-Gaussian continuum mechanics, different balance laws for forces and solvent (including diffusion), and the thermodynamics of mixing. Including energy, diffusion, and hyperelastic terms, this new model can be used for both constrained and free swelling. Boundary conditions for free swelling are incorporated into the model. A MATLAB code is then developed for model solution. New experiments have been performed to determine input values such as viscosity of swelling medium and polymer-solvent interaction parameter. Stretch values predicted by the model are used to determine volume and thickness swelling, and variation of shear modulus. Model predictions have good agreement with experimental results, much closer than numerical simulation based on best existing hyperelastic material model.

IntechOpen

### **Author details**

Sayyad Zahid Qamar<sup>1\*</sup>, Maaz Akhtar<sup>2</sup> and Tasneem Pervez<sup>1</sup>

1 Mechanical and Industrial Engineering Department, Sultan Qaboos University, Muscat, Oman

2 Mechanical Engineering Department, N.E.D. University of Engineering and Technology, Karachi, Pakistan

\*Address all correspondence to: sayyad@squ.edu.om

### **IntechOpen**

---

© 2021 The Author(s). Licensee IntechOpen. Distributed under the terms of the Creative Commons Attribution - NonCommercial 4.0 License (<https://creativecommons.org/licenses/by-nc/4.0/>), which permits use, distribution and reproduction for non-commercial purposes, provided the original is properly cited. 

## References

- [1] Akhtar M, Qamar SZ, Pervez T, Al-Jahwari FK (2018) "Performance Analysis of Swelling Elastomer Seals," *Petroleum Science and Engineering*, 165 (2018), p 127–135
- [2] Okumura D, Chester SA (2018) "Ultimate swelling described by limiting chain extensibility of swollen elastomers," *International Journal of Mechanical Sciences*, 144, p 531–539
- [3] Landsgesell J, Sean D, Kreissl P, Szuttor K, Holm C (2019) "Modeling Gel Swelling Equilibrium in the Mean Field: From Explicit to Poisson-Boltzmann Models," *Physical Review Letters*, 122, 208002
- [4] Hong W, Liu Z, Suo Z (2009) "Inhomogeneous Swelling of a Gel in Equilibrium with a Solvent and Mechanical Load, *International Journal of Solids and Structures*, 46(17), 3282–3289
- [5] Hong W, Zhao X, Zhou J, Suo Z (2008) "A Theory of Coupled Diffusion and Large Deformation in Polymeric Gels," *Journal of the Mechanics and Physics of Solids*, 56(5), 1779–1793
- [6] Kang MK, Huang R (2010) "A Variational Approach and Finite Element Implementation for Swelling of Polymeric Hydrogels under Geometric Constraints," *Journal of Applied Mechanics*, 77(6), 061004
- [7] Lucantonio A, Nardinocchi P, Teresi L (2013) "Transient Analysis of Swelling-Induced Large Deformations in Polymer Gels," *Journal of the Mechanics and Physics of Solids*, 61(1), 205–218
- [8] Treloar LRG (1975) *The Physics of Rubber Elasticity*, Oxford University Press
- [9] Ogden R (1972) "Large Deformation Isotropic Elasticity — On the Correlation of Theory and Experiment for Incompressible Rubberlike Solids," *Proceedings of the Royal Society of London. A. Mathematical and Physical Sciences*, 326(1567), 565–584
- [10] Chester SA, Anand L (2010) "A Coupled Theory of Fluid Permeation and Large Deformations for Elastomeric Materials," *Journal of the Mechanics and Physics of Solids*, 58(11), 1879–1906
- [11] Flory PJ (1953) *Principles of Polymer Chemistry*, Cornell University Press
- [12] Crank J (1979) *The Mathematics of Diffusion*, Oxford University Press
- [13] Doi M (2009) "Gel Dynamics," *Journal of the Physical Society of Japan*, 78(5)
- [14] Mase GT, Mase GE (2010) *Continuum Mechanics for Engineers*, CRC Press
- [15] Bucalem ML, Bathe K-J (2011) *The Mechanics of Solids and Structures: Hierarchical Modeling and the Finite Element Solution*, Springer
- [16] Gurtin ME, Fried E, Anand L (2010) *The Mechanics and Thermodynamics of Continua*, Cambridge University Press
- [17] Frémond M (2006) "The Clausius-Duhem Inequality, an Interesting and Productive Inequality," in: Alart P, Maisonneuve O, Rockafellar RT (eds) *Nonsmooth Mechanics and Analysis. Advances in Mechanics and Mathematics*, vol 12. Springer, Boston
- [18] Drozdov A, Christiansen J (2013) "Constitutive Equations in Finite Elasticity of Swollen Elastomers," *International Journal of Solids and Structures*, 50(9), 1494–1504

- [19] Biot MA (1941) "General Theory of Three-Dimensional Consolidation," *Journal of Applied Physics*, 12, 155–164
- [20] Tanaka T, Fillmore DJ (1979) "Kinetics of Swelling Gels," *Journal of Chemical Physics*, 70(3), 1214
- [21] Feynman R, Leighton R, Sands M (1963) *The Feynman Lectures on Physics*, Addison-Wesley
- [22] Huggins ML (1942) "Some Properties of Solutions of Long-Chain Compounds," *The Journal of Physical Chemistry*, 46(1), 151–158
- [23] Flory PJ (1942) "Thermodynamics of High Polymer Solutions," *Journal of Chemical Physics*, 10, 51–61
- [24] Duda FP, Souza AC, Fried E (2010) "A Theory for Species Migration in a Finitely Strained Solid with Application to Polymer Network Swelling," *Journal of the Mechanics and Physics of Solids*, 58(4), 515–529
- [25] Flory P, Rehner J (1943) "Statistical Mechanics of Cross-Linked Polymer Networks: I. Swelling," *Journal of Chemical Physics*, 11, 521–526
- [26] Einstein A (1905) "On the Movement of Small Particles Suspended in Stationary Liquids Required by the Molecular-Kinetic Theory of Heat," *Annalen der Physik*, 17 (1905), 549–560
- [27] Cannon M, Fenske M (1938) "Viscosity Measurement," *Industrial & Engineering Chemistry Analytical Edition*, 10(6), 297–301
- [28] Orwoll RA, Arnold PA (2007) "Polymer–Solvent Interaction Parameter  $\chi$ ," in JE Mark (ed) *Physical Properties of Polymers Handbook*, p 233–257, Springer, New York
- [29] Papageorgiou GZ, Panayiotou C (2011) "Crystallization and Melting of Biodegradable Poly(propylene suberate)," *Thermochimica Acta*, 523 (1–02), p 187–199
- [30] Silva L, Tognana S, Salgueiro W (2013) "Miscibility in Crystalline/Amorphous Blends of Poly(3-hydroxybutyrate)/DGEBA," *Journal of Polymer Science, Part B: Polymer Physics*, 51, 680–686
- [31] Clarke CJ, Eisenberg A, La Scala J, Rafailovich MH, Sokolov J, Li Z, Qu S, Nguyen D, Schwarz SA, Strzhemechny Y, Sauer BB (1997) "Measurements of the Flory–Huggins Interaction Parameter for Polystyrene–Poly(4-vinylpyridine) Blends," *Macromolecules*, 30, 14, 4184–4188